Robust Adaptive Nonlinear Dynamic Inversion Control for an Air-breathing Hypersonic Vehicle

Guanghui Wu , Xiuyun Meng and Jie Wang

School of Aerospace Engineering, Beijing Institute of Technology, 100081, Beijing, China

Abstract. This paper presents a robust adaptive nonlinear dynamic inversion control approach for the longitudinal dynamics of an air-breathing hypersonic vehicle. The proposed approach adopts a fast adaptation law using high-gain learning rate, while a low-pass filter is synthesized with the modified adaptive scheme to filter out the high-frequency content of the estimates. This modified high-gain adaptive scheme achieves a good transient process and a nice robust property with respect to parameter uncertainties, without exciting high-frequency oscillations. Based on input-output linearization, the nonlinear hypersonic dynamics are transformed into equivalent linear systems. Therefore, the pole placement technique is applied to design the baseline nonlinear dynamic inversion controller. Finally, the simulation results of the modified adaptive nonlinear dynamic inversion control law demonstrate the proposed control approach provides robust tracking of reference trajectories.

1 Introduction

Since the winged-cone hypersonic vehicle model [1] was presented by NASA Langley Research Center, the air-breathing hypersonic vehicles (AHVs) have attracted much interest around the world. What's more, the successful flight of X-43A [2], X-51A, and Hyshot2 [3] has given a great number of test data on the aerodynamics, structure, guidance, and control of AHVs, enriching the knowledge of hypersonic theory. However, the highly coupled dynamics make the AHVs sensitive to flight condition [4]. As a result, a robust control system is important to the AHVs.

The feedback linearization method has been widely used in AHVs. Wang and Stengel [5] gave the condition of applying nonlinear dynamic inversion (NDI) for a generic AHV. In their work, the nonlinear vehicle systems were transformed into equivalent linear systems. Afterward, the genetic algorithm was applied to optimize the design parameters of the LQR control. But the feedback linearization requires an accurate model because it's sensitive to uncertainties. To enhance the robustness of the NDI control, Xu et al. [6] adopted sliding mode control to design a NDI controller for the AHV. In parker [7], the elevator-to-lift coupling was canceled by adding an additional canard. What's more, adaptive technique is synthesized with the feedback linearization method. Chen and Ai [8] proposed a NDI based L1 adaptive control design for the AHV. The L1 adaptive term was used to estimate the parametric uncertainties and external disturbances. Fiorentini et al. [9] applied the canard deflection to control the outer-loop and utilized the elevator deflection to control the inner-loop, resulting in low-order subsystems. Based on these low-order subsystems, a robust adaptive dynamic inversion approach was implemented to achieve robust tracking performance.

In this study, the canard included [7, 9] configuration is adopted to create low-order subsystems. Based on NID, the nonlinear systems are transformed into low-order linear subsystems. We applied the pole placement method [10] to design the control parameters of the equivalent linear systems. To enhance the stability of the control system, a modified adaptive scheme [11] was applied to estimate the parametric uncertainty. In the adaptive term, a low-pass filter was introduced to the estimate parameters. As a result, the high frequency content of the adaptive process is canceled. In the end, Monet Carlo simulation was conducted to demonstrate the robustness of the proposed method.

The main contributions of this study are: (a) with an additional canard, the relative degree of the system is well defined without dynamic extension; (b) the pole placement technique is synthesized with the NDI to design the feedback gains of the equivalent linear system; (c) the modified adaptive scheme is adopted to improve the performance of the AHV. The remainder of this paper is organized as follows: In Sec. 2, a nonlinear model of the AHV is presented and the control-oriented equations are obtained. The control design of the NDI is proposed in Sec. 3. Finally, simulation results and conclusions are presented in Sec.4 and Sec. 5, respectively.

2 Model description

In this study, the longitudinal model is based on Bolender and Doman [4]. The longitudinal dynamic equations of an AHV are

$$\dot{V} = \left(T\cos\alpha - D\right)/m - g\sin\gamma \tag{1}$$

$$\dot{h} = V\sin\gamma \tag{2}$$

$$\dot{\gamma} = \left(L + T\sin\alpha\right)/\left(mV\right) - g\cos\gamma/V \tag{3}$$

$$\dot{\theta} = q \tag{4}$$

$$\dot{q} = M/I_{yy} \tag{5}$$

The model comprises five states $\boldsymbol{x} = [V,\ h,\ \gamma,\ \theta,\ q]^T$, where V is the velocity, h is the altitude, γ is the flight path angle, θ is the pitch angle, and q is the pitch rate. The angle of attack is given by $\alpha = \theta - \gamma$. The control inputs $\boldsymbol{u} = [\phi,\ \delta_e,\ \delta_c]^T$ and the regulated outputs $[V,\ h,\ \theta]^T$ form a three inputs and three outputs system, where ϕ is the equivalent fuel-to-air ratio, δ_e is the elevator deflection, and δ_c is the canard deflection. The control object is to asymptotically track the reference trajectories of velocity, altitude, and pitch angel. The 50% fuel level [12] is defined as the nominal operating condition.

In the curve-fitted model, the lift L, drag D, thrust T, and pitching moment M are given by

$$\begin{aligned} T &\approx \bar{q}S\left[C_{T,\phi}\left(\alpha\right)\phi + C_T\left(\alpha\right)\right] \\ L &\approx \bar{q}SC_L\left(\alpha,\boldsymbol{\delta}\right) \\ D &\approx \bar{q}SC_D\left(\alpha,\boldsymbol{\delta}\right) \\ M &\approx z_T T + \bar{q}S\bar{c}C_M\left(\alpha,\boldsymbol{\delta}\right) \end{aligned} \tag{6}$$

where, $\bar{q}$, S, $\bar{c}$ and z_T are the dynamic pressure, reference area, mean aerodynamic chord, and thrust moment arm, respectively. The dynamic pressure is expressed as $\bar{q} = 0.5\rho V^2$, while the air density is given by $\rho = \rho_0\exp[-(h-h_0)/h_s]$. The aerodynamic coefficients, mass and the moment of inertia are present by

$$\begin{aligned} &\boldsymbol{\delta} = \left[\delta_e,\delta_c\right]^T \\ &C_{T,\phi}\left(\alpha\right) = \nu_1 C_T^{\phi\alpha^3}\alpha^3 + \nu_2 C_T^{\phi\alpha^2}\alpha^2 + \nu_3 C_T^{\phi\alpha}\alpha + \nu_4 C_T^{\phi} \\ &C_T\left(\alpha\right) = \nu_5 C_T^3\alpha^3 + \nu_6 C_T^2\alpha^2 + \nu_7 C_T^1\alpha + \nu_8 C_T^0 \\ &C_L\left(\alpha,\boldsymbol{\delta}\right) = \nu_9 C_L^{\alpha}\alpha + \nu_{10} C_L^{\delta_e}\delta_e + \nu_{11} C_L^{\delta_c}\delta_c + \nu_{12} C_L^0 \\ &C_D\left(\alpha,\boldsymbol{\delta}\right) = \nu_{13} C_D^{\alpha^2}\alpha^2 + \nu_{14} C_D^{\alpha}\alpha + \nu_{15} C_D^0 \\ &C_M\left(\alpha,\boldsymbol{\delta}\right) = \nu_{16} C_M^{\alpha^2}\alpha^2 + \nu_{17} C_M^{\alpha}\alpha + \nu_{18} C_M^{\delta_e}\delta_e + \\ &\qquad \nu_{19} C_M^{\delta_c}\delta_c + \nu_{20} C_M^0 \\ &m = \nu_{21} m_0 \\ &I_{yy} = \nu_{22} I_{yy0} \end{aligned} \tag{7}$$

where the parameters ν_i, i = 1, 2, …, 22, are modeled as parametric uncertainty, and the numerical values of the curve-fitted coefficients and the vehicle parameters can be found in Fiorentini [13].

In order to apply the NDI control, the sum of the relative degree in each subsystem is required to equal the order of the system dynamics. The dynamics of actuators are neglected in controller design to meet the requirement of the relative degree. The system was divided into functional subsystems that are the velocity subsystem, altitude subsystem, and pitch angle subsystem. Due to the small effect of elevator and canard on velocity, the velocity subsystem is decoupled from the other two subsystems. For altitude and pitch angle subsystems, the control inputs become the elevator and canard deflection. The initial trim condition is shown in Table 1. The control-oriented equations are expressed as follows.

Table 1. The initial trim condition.

State	Value	Input	Value
V	2392.7 m/s	ϕ	0.2
h	25908 m	δ_e	0.081 rad
γ	0 rad	δ_c	−0.081rad
θ	0.0292 rad		
Q	0 rad/s		

$$\dot{V} = \theta_1^T\varphi_1 + \theta_2^T\varphi_2\phi - g\sin\gamma \tag{8}$$

$$\begin{aligned} \dot{h} &= V\sin\gamma \\ \ddot{h} &= \theta_3^T\varphi_3 + \theta_4^T\varphi_4\delta - g \end{aligned} \tag{9}$$

$$\begin{aligned} \dot{\theta} &= q \\ \ddot{\theta} &= \theta_5^T\varphi_5 + \theta_6^T\varphi_6\delta \end{aligned} \tag{10}$$

The detailed expressions of the functions

$$\begin{aligned} \theta_1 &= \left(1/\nu_{21}\right)\left[\nu_5,\nu_6,\nu_7,\nu_8,\nu_{13},\nu_{14},\nu_{15}\right]^T \\ \varphi_1 &= \left(\bar{q}S/m_0\right)[\alpha^3\cos\alpha C_T^3,\alpha^2\cos\alpha C_T^2,\alpha\cos\alpha C_T^1, \\ &\qquad \cos\alpha C_T^0,-\alpha^2 C_D^{\alpha^2},-\alpha C_D^{\alpha},-C_D^0]^T \\ \theta_2 &= \left(1/\nu_{21}\right)\left[\nu_1,\nu_2,\nu_3,\nu_4\right]^T \\ \varphi_2 &= \left(\bar{q}S\cos\alpha/m_0\right)\left[\alpha^3 C_T^{\phi\alpha^3},\alpha^2 C_T^{\phi\alpha^2},\alpha C_T^{\phi\alpha},C_T^{\phi}\right]^T \end{aligned}$$

$$\begin{aligned} \theta_3 &= \left(1/\nu_{21}\right)\left[\nu_1,\nu_2,\nu_3,\nu_4,\nu_5,\nu_6,\nu_7,\nu_8,\nu_{13},\nu_{14},\nu_{15},\nu_9,\nu_{12}\right]^T \\ \varphi_3 &= \left(\bar{q}S/m_0\right)[\alpha^3\phi\sin\theta C_T^{\phi\alpha^3},\alpha^2\phi\sin\theta C_T^{\phi\alpha^2},\alpha\phi\sin\theta C_T^{\phi\alpha}, \\ &\qquad \phi\sin\theta C_T^{\phi},\alpha^3\sin\theta C_T^3,\alpha^2\sin\theta C_T^2,\alpha\sin\theta C_T^1,\sin\theta C_T^0, \\ &\qquad -\alpha^2\sin\gamma C_D^{\alpha^2},-\alpha\sin\gamma C_D^{\alpha},-\sin\gamma C_D^0,\alpha\cos\gamma C_L^{\alpha}, \\ &\qquad \cos\gamma C_L^0]^T \end{aligned}$$

$$\begin{aligned} \theta_4 &= \left(1/\nu_{20}\right)\left[\nu_{10},\nu_{11}\right]^T \\ \varphi_4 &= \left(\bar{q}S\cos\gamma/m_0\right)diag\left(C_L^{\delta_e},C_L^{\delta_c}\right) \end{aligned}$$

$$\begin{aligned} \theta_5 &= \left(1/\nu_{22}\right)\left[\nu_1,\nu_2,\nu_3,\nu_4,\nu_5,\nu_6,\nu_7,\nu_8,\nu_{16},\nu_{17},\nu_{20}\right]^T \\ \varphi_5 &= \left(\bar{q}S/I_{yy0}\right)[z_T\alpha^3\phi C_T^{\phi\alpha^3},z_T\alpha^2\phi C_T^{\phi\alpha^2},z_T\alpha\phi C_T^{\phi\alpha}, \\ &\qquad z_T\phi C_T^{\phi},z_T\alpha^3 C_T^3,z_T\alpha^2 C_T^2,z_T\alpha C_T^1,z_T C_T^0,\bar{c}\alpha^2 C_M^{\alpha^2}, \\ &\qquad \bar{c}\alpha C_M^{\alpha},\bar{c}C_M^0]^T \end{aligned}$$

$$\theta_6 = (1/\nu_{22})[\nu_{18}, \nu_{19}]^T$$
$$\varphi_6 = (\bar{q}S\bar{c}/I_{yy0})\, diag(C_M^{\delta_e}, C_M^{\delta_c})$$

3. Control design

The equations of motion are decomposed into functional systems that are the velocity subsystem, altitude subsystem, and pitch angle subsystem. Based on input-output linearization, each subsystem is transformed into an equivalent linear system. Based on the linear systems, the pole placement technique is applied to design the feedback gains. To enhance the robustness of the control system, the modified adaptive scheme is adopted to estimate the parametric uncertainty.

3.1 NDI control for the velocity subsystem

Define the velocity tracking error

$$\tilde{V} = V - V_{ref} \tag{11}$$

The tracking error dynamics of velocity become

$$\dot{\tilde{V}} = \theta_1^T \varphi_1 + \theta_2^T \varphi_2 \phi - g\sin\gamma - \dot{V}_{ref} \tag{12}$$

By dynamic inversion, the command of the equivalent fuel-to-air ratio is designed as

$$\phi = \left(-k_{PV}\tilde{V} - \hat{\theta}_1^T \varphi_1 + g\sin\gamma + \dot{V}_{ref}\right) / \left(\hat{\theta}_2^T \varphi_2\right) \tag{13}$$

where, k_{PV} is a positive constant, and $\hat{\theta}_1$ and $\hat{\theta}_2$ are the estimates of θ_1 and θ_2. The modified adaptation law is designed as

$$\dot{\hat{\theta}}_1 = \Gamma_1 \,\mathrm{Proj}\left(\tilde{V}\varphi_1 - \sigma_1\left(\hat{\theta}_1 - \hat{\theta}_{1f}\right)\right) \tag{14}$$

$$\dot{\hat{\theta}}_2 = \Gamma_2 \,\mathrm{Proj}\left(\tilde{V}\varphi_2 \phi - \sigma_2\left(\hat{\theta}_2 - \hat{\theta}_{2f}\right)\right) \tag{15}$$

The Proj(·) is a projection operator [14], and it follows the definition [15]

$$-\tilde{\theta}_i\left(\mathrm{Proj}(y) - y\right) \le 0; i = 1, 2, ...6 \tag{16}$$

The adaptive gains are Γ_1 and Γ_2, the filtered estimates are $\hat{\theta}_{3f}$ and $\hat{\theta}_{4f}$, and the damping gains are σ_1 and σ_2. The detailed description of the filtered estimates is

$$\dot{\hat{\theta}}_{1f} = \Gamma_{1f}\left(\hat{\theta}_1 - \hat{\theta}_{1f}\right) \tag{17}$$

$$\dot{\hat{\theta}}_{2f} = \Gamma_{2f}\left(\hat{\theta}_2 - \hat{\theta}_{2f}\right) \tag{18}$$

where Γ_{1f} and Γ_{2f} present the desired crossover frequencies. Therefore, the filter cuts off the high frequency content of the estimates.

Define the estimation errors

$$\tilde{\theta}_i = \theta_i - \hat{\theta}_i; \tilde{\theta}_{if} = \theta_i - \hat{\theta}_{if}; i = 1, 2, ..., 6 \tag{19}$$

The tracking error dynamics of velocity are

$$\dot{\tilde{V}} = -k_{PV}\tilde{V} + \tilde{\theta}_1^T \varphi_1 + \tilde{\theta}_2^T \varphi_2 \phi \tag{20}$$

Choose the Lyapunov function

$$W_V = \tilde{V}^2/2 + \tilde{\theta}_1^T \Gamma_1^{-1} \tilde{\theta}_1/2 + (\sigma_1/2)\tilde{\theta}_{1f}^T \Gamma_{1f}^{-1} \tilde{\theta}_{1f} + \tilde{\theta}_2^T \Gamma_2^{-1} \tilde{\theta}_2/2 + (\sigma_2/2)\tilde{\theta}_{2f}^T \Gamma_{2f}^{-1} \tilde{\theta}_{2f} \tag{21}$$

The derivative of the Lyapunov function candidate W_V is

$$\begin{aligned}
\dot{W}_V &= -k_{PV}\tilde{V}^2 + \tilde{V}\tilde{\theta}_1^T \varphi_1 + \tilde{V}\tilde{\theta}_2^T \varphi_2 \phi - \tilde{\theta}_1^T \Gamma_1^{-1} \dot{\hat{\theta}}_1 - \sigma_1 \tilde{\theta}_{1f}^T \Gamma_{1f}^{-1} \dot{\hat{\theta}}_{1f} - \\
&\quad \tilde{\theta}_2^T \Gamma_2^{-1} \dot{\hat{\theta}}_2 - \sigma_2 \tilde{\theta}_{2f}^T \Gamma_{2f}^{-1} \dot{\hat{\theta}}_{2f} \\
&= -k_{PV}\tilde{V}^2 + \tilde{V}\tilde{\theta}_1^T \varphi_1 + \tilde{V}\tilde{\theta}_2^T \varphi_2 \phi - \tilde{\theta}_1^T \,\mathrm{Proj}\left(\tilde{V}\varphi_1 - \sigma_1\left(\tilde{\theta}_{1f} - \tilde{\theta}_1\right)\right) - \\
&\quad \sigma_1 \tilde{\theta}_{1f}^T \left(\tilde{\theta}_{1f} - \tilde{\theta}_1\right) - \tilde{\theta}_2^T \,\mathrm{Proj}\left(\tilde{V}\varphi_2 \phi - \sigma_2\left(\tilde{\theta}_{2f} - \tilde{\theta}_2\right)\right) - \\
&\quad \sigma_2 \tilde{\theta}_{2f}^T \left(\tilde{\theta}_{2f} - \tilde{\theta}_2\right) \\
&= -k_{PV}\tilde{V}^2 + \tilde{V}\tilde{\theta}_1^T \varphi_1 - \sigma_1 \tilde{\theta}_1^T \left(\tilde{\theta}_{1f} - \tilde{\theta}_1\right) - \sigma_1 \left(\tilde{\theta}_{1f} - \tilde{\theta}_1\right)^T \left(\tilde{\theta}_{1f} - \tilde{\theta}_1\right) - \\
&\quad \tilde{\theta}_1^T \,\mathrm{Proj}\left(\tilde{V}\varphi_1 - \sigma_1\left(\tilde{\theta}_{1f} - \tilde{\theta}_1\right)\right) + \tilde{V}\tilde{\theta}_2^T \varphi_2 \phi - \sigma_2 \tilde{\theta}_2^T \left(\tilde{\theta}_{2f} - \tilde{\theta}_2\right) - \\
&\quad \tilde{\theta}_2^T \,\mathrm{Proj}\left(\tilde{V}\varphi_2 \phi - \sigma_2\left(\tilde{\theta}_{2f} - \tilde{\theta}_2\right)\right) - \sigma_2 \left(\tilde{\theta}_{2f} - \tilde{\theta}_2\right)^T \left(\tilde{\theta}_{2f} - \tilde{\theta}_2\right) \\
&\le -k_{PV}\tilde{V}^2 - \sigma_1 \left(\tilde{\theta}_{1f} - \tilde{\theta}_1\right)^T \left(\tilde{\theta}_{1f} - \tilde{\theta}_1\right) - \sigma_2 \left(\tilde{\theta}_{2f} - \tilde{\theta}_2\right)^T \left(\tilde{\theta}_{2f} - \tilde{\theta}_2\right) \\
&\le 0
\end{aligned} \tag{22}$$

3.2 NDI control for the altitude and pitch subsystems

Define the altitude tracking error

$$\tilde{h} = h - h_{ref}; \dot{\tilde{h}} = V\sin\gamma - \dot{h}_{ref} \tag{23}$$

The tracking error dynamics of altitude become

$$\ddot{\tilde{h}} = \theta_3^T \varphi_3 + \theta_4^T \varphi_4 \delta - g - \ddot{h}_{ref} \tag{24}$$

By dynamic inversion, design the virtual control signal

$$u_h = \hat{\theta}_4^T \varphi_4 \delta = -k_{Ph}\tilde{h} - k_{Dh}\dot{\tilde{h}} - \hat{\theta}_3^T \varphi_3 + g + \ddot{h}_{ref} \tag{25}$$

where, k_{Ph} and k_{Dh} are positive constants, and $\hat{\theta}_3$ and $\hat{\theta}_4$ are the estimates of θ_3 and θ_4. The tracking error dynamics become

$$\begin{bmatrix} \dot{\tilde{h}} \\ \ddot{\tilde{h}} \end{bmatrix} = \underbrace{\begin{bmatrix} 0 & 1 \\ -k_{Ph} & -k_{Dh} \end{bmatrix}}_{A_h} \begin{bmatrix} \tilde{h} \\ \dot{\tilde{h}} \end{bmatrix} + \underbrace{\begin{bmatrix} 0 \\ 1 \end{bmatrix}}_{b_h} \left(\tilde{\theta}_3^T \varphi_3 + \tilde{\theta}_4^T \varphi_4 \delta\right) \tag{26}$$

Define the extended tracking error of altitude subsystem

$$e_h = [\tilde{h}, \dot{\tilde{h}}]^T \tag{27}$$

The modified adaptation law is designed as

$$\dot{\hat{\theta}}_3 = \Gamma_3 \,\mathrm{Proj}\left(\varphi_3 e_h^T Pb - \sigma_3\left(\hat{\theta}_3 - \hat{\theta}_{3f}\right)\right) \tag{28}$$

$$\dot{\hat{\theta}}_4 = \Gamma_4 \,\mathrm{Proj}\left(\varphi_4 \delta e_h^T Pb - \sigma_4\left(\hat{\theta}_4 - \hat{\theta}_{4f}\right)\right) \tag{29}$$

where the adaptive gains are Γ_3 and Γ_4. The filtered estimates are $\hat{\theta}_{3f}$ and $\hat{\theta}_{4f}$, and the damping gains are σ_3 and σ_4. The detailed description of the filtered estimates is

$$\dot{\hat{\theta}}_{3f} = \Gamma_{3f}\left(\hat{\theta}_3 - \hat{\theta}_{3f}\right) \tag{30}$$

$$\dot{\hat{\theta}}_{4f} = \Gamma_{4f}\left(\hat{\theta}_4 - \hat{\theta}_{4f}\right) \tag{31}$$

where Γ_{3f} and Γ_{4f} present the desired crossover frequencies. Choose a symmetric positive-definite matrix $Q_h = I_2$ and solve the following algebraic Lyapunov equation:

$$P_h A_h + A_h^T P_h = -Q_h \tag{32}$$

Define the Lyapunov function in this subsystem

$$\begin{aligned} W_h = {} & e_h^T P_h e_h / 2 + \tilde{\theta}_3^T \Gamma_3^{-1} \tilde{\theta}_3 / 2 + (\sigma_3 / 2)\tilde{\theta}_{3f}^T \Gamma_{3f}^{-1} \tilde{\theta}_{3f} + \\ & \tilde{\theta}_4^T \Gamma_4^{-1} \tilde{\theta}_4 / 2 + (\sigma_4 / 2)\tilde{\theta}_{4f}^T \Gamma_{4f}^{-1} \tilde{\theta}_{4f} \end{aligned} \tag{33}$$

Similar to (22), the derivative of the Lyapunov function candidate W_h is

$$\begin{aligned} \dot{W}_h = {} & -e_h^T Q_h e_h / 2 + e_h^T P_h b_h \left(\tilde{\theta}_3^T \varphi_3 + \tilde{\theta}_4^T \varphi_4 \delta\right) - \tilde{\theta}_3^T \Gamma_3^{-1} \dot{\hat{\theta}}_3 - \\ & \sigma_3 \tilde{\theta}_{3f}^T \Gamma_{3f}^{-1} \dot{\hat{\theta}}_{3f} - \tilde{\theta}_4^T \Gamma_4^{-1} \dot{\hat{\theta}}_4 - \sigma_4 \tilde{\theta}_{4f}^T \Gamma_{4f}^{-1} \dot{\hat{\theta}}_{4f} \\ \le {} & -e_h^T Q_h e_h / 2 - \sigma_3 \left(\tilde{\theta}_{3f} - \tilde{\theta}_3\right)^T \left(\tilde{\theta}_{3f} - \tilde{\theta}_3\right) - \\ & \sigma_4 \left(\tilde{\theta}_{4f} - \tilde{\theta}_4\right)^T \left(\tilde{\theta}_{4f} - \tilde{\theta}_4\right) \\ \le {} & 0 \end{aligned} \tag{34}$$

Define the pitch angle tracking error

$$\tilde{\theta} = \theta - \theta_{ref}; \dot{\tilde{\theta}} = q - \dot{\theta}_{ref} \tag{35}$$

The tracking error dynamics of altitude become

$$\ddot{\tilde{\theta}} = \theta_5^T \varphi_5 + \theta_6^T \varphi_6 \delta - \ddot{\theta}_{ref} \tag{36}$$

By dynamic inversion, design the virtual control signal

$$u_\theta = \hat{\theta}_6^T \varphi_6 \delta = -k_{P\theta}\tilde{\theta} - k_{D\theta}\dot{\tilde{\theta}} - \hat{\theta}_5^T \varphi_5 + \ddot{\theta}_{ref} \tag{37}$$

where, $k_{P\theta}$ and $k_{D\theta}$ are positive constants, and $\hat{\theta}_5$ and $\hat{\theta}_6$ are the estimates of θ_5 and θ_6. The tracking error dynamics become

$$\begin{bmatrix} \dot{\tilde{\theta}} \\ \ddot{\tilde{\theta}} \end{bmatrix} = \underbrace{\begin{bmatrix} 0 & 1 \\ -k_{P\theta} & -k_{D\theta} \end{bmatrix}}_{A_\theta} \begin{bmatrix} \tilde{\theta} \\ \dot{\tilde{\theta}} \end{bmatrix} + \underbrace{\begin{bmatrix} 0 \\ 1 \end{bmatrix}}_{b_\theta} \left(\tilde{\theta}_5^T \varphi_5 + \tilde{\theta}_6^T \varphi_6 \delta\right) \tag{38}$$

Define the extended tracking error of the altitude subsystem

$$e_\theta = [\tilde{\theta}, \dot{\tilde{\theta}}]^T \tag{39}$$

The modified adaptation law is designed as

$$\dot{\hat{\theta}}_5 = \Gamma_5 \,\mathrm{Proj}\left(\varphi_5 e_\theta^T Pb - \sigma_5\left(\hat{\theta}_5 - \hat{\theta}_{5f}\right)\right) \tag{40}$$

$$\dot{\hat{\theta}}_6 = \Gamma_6 \,\mathrm{Proj}\left(\varphi_6 \delta e_\theta^T Pb - \sigma_6\left(\hat{\theta}_6 - \hat{\theta}_{6f}\right)\right) \tag{41}$$

where the adaptive gains are Γ_5 and Γ_6. The filtered estimates are $\hat{\theta}_{5f}$ and $\hat{\theta}_{6f}$, and the damping gains are σ_5 and σ_6. The detailed description of the filtered estimates is

$$\dot{\hat{\theta}}_{5f} = \Gamma_{5f}\left(\hat{\theta}_5 - \hat{\theta}_{5f}\right) \tag{42}$$

$$\dot{\hat{\theta}}_{6f} = \Gamma_{6f}\left(\hat{\theta}_6 - \hat{\theta}_{6f}\right) \tag{43}$$

Choose a symmetric positive-definite matrix $Q_\theta = I_2$ and solve the following algebraic Lyapunov equation:

$$P_\theta A_\theta + A_\theta^T P_\theta = -Q_\theta \tag{44}$$

Define the Lyapunov function

$$\begin{aligned} W_\theta = {} & e_\theta^T P_\theta e_\theta / 2 + \tilde{\theta}_5^T \Gamma_5^{-1} \tilde{\theta}_5 / 2 + (\sigma_5 / 2)\tilde{\theta}_{5f}^T \Gamma_{5f}^{-1} \tilde{\theta}_{5f} + \\ & \tilde{\theta}_6^T \Gamma_6^{-1} \tilde{\theta}_6 / 2 + (\sigma_6 / 2)\tilde{\theta}_{6f}^T \Gamma_{6f}^{-1} \tilde{\theta}_{6f} \end{aligned} \tag{45}$$

Similarly, the derivative of the Lyapunov function candidate W_θ is

$$\begin{aligned} \dot{W}_\theta \le {} & -e_\theta^T Q_\theta e_\theta / 2 - \sigma_5 \left(\tilde{\theta}_{5f} - \tilde{\theta}_5\right)^T \left(\tilde{\theta}_{5f} - \tilde{\theta}_5\right) - \\ & \sigma_6 \left(\tilde{\theta}_{6f} - \tilde{\theta}_6\right)^T \left(\tilde{\theta}_{6f} - \tilde{\theta}_6\right) \\ \le {} & 0 \end{aligned} \tag{46}$$

Define the matrix

$$G(x) = \left[\hat{\theta}_4^T \varphi_4, \hat{\theta}_6^T \varphi_6\right]^T \tag{47}$$

The determinant of $G(\boldsymbol{x})$ is

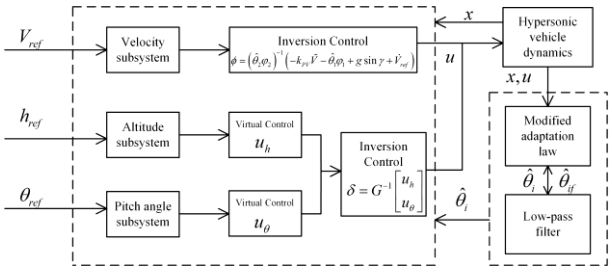

Figure 1. Block diagram of the modified adaptive NDI control design.

$$\det\left(G(x)\right) = V\cos\gamma\bar{q}^2S^2\bar{c}\cdot \left(\nu_{10}\nu_{19}C_M^{\delta_c}C_L^{\delta_e} - \nu_{11}\nu_{18}C_M^{\delta_e}C_L^{\delta_c}\right)/ \left(\nu_{21}\nu_{22}mVI_{yy}\right) \quad (48)$$

Equation (48) shows $G(\boldsymbol{x})$ is nonsingular. By dynamic inversion, the command of the elevator and canard is

$$\boldsymbol{\delta} = G^{-1}\left[u_h, u_\theta\right]^T \quad (49)$$

In conclusion, the commands of the inputs are derived in (13) and (49). The block diagram of the modified adaptive NDI control system is presented in Fig. 1.

3.3 Pole placement technique

Equations (20), (26) and (38) show the nonlinear vehicle dynamics are transformed into equivalent linear systems. We apply pole placement technique to design the feedback gains. Take the pitch angle subsystem as an example. The pitch angle subsystem is transformed into a typical second-order system, and the feedback gains of the second-order system is designed as

$$k_{P\theta} = \omega_n^2, k_{D\theta} = 2\zeta_n\omega_n \quad (50)$$

where the damping ratio ζ_n is designed to achieve good transient performance, and the natural frequency ωn is set to guarantee a suitable bandwidth of the closed-loop system.

Based on this part, the equivalent systems have been designed. The real pole p of the velocity subsystem is designed as $p = -5$. In the altitude subsystem, the natural frequency is designed as $\omega_n = 2$ rad/s, and the damping ratio is 0.75. In the pitch angle subsystem, the natural frequency is 6 rad/s, and the damping ratio is 1.25. It's noted that, the pitch angle subsystem is over-damped.

Table 2. Admissible of the range of the variables

Variable	Minimum value	Maximum value
V, m/s	2286	3413.7
h, m	21336	41148
γ , deg	-3	3
α, deg	-5	10
Q, deg/s	-10	10
δ, deg	-20	20
ϕ	0.05	1.5

Table 3. control parameters

Subsystem	gain	Adaptive gain	Filter gain
Velocity	$k_{pV} = 5$	$\Gamma_1 = 1I_7$, $\sigma_1 = 10$, $\Gamma_2 = 1I_4$, $\sigma_2 = 10$	$\Gamma_{1f} = 5I_7$ $\Gamma_{2f} = 5I_4$
Altitude	$k_{ph} = 4$ $k_{dh} = 3$	$\Gamma_3 = 1I_{13}$, $\sigma_3 = 50$, $\Gamma_4 = 1I_2$, $\sigma_4 = 50$	$\Gamma_{3f} = 2I_{13}$ $\Gamma_{4f} = 2I_2$
Pitch	$k_{p\theta} = 36$ $k_{d\theta} = 15$	$\Gamma_5 = 1e3I_{11}$, $\sigma_5 = 0.02$, $\Gamma_6 = 1e2I_2$, $\sigma_6 = 0.02$	$\Gamma_{5f} = 6I_{11}$ $\Gamma_{6f} = 6I_2$

4. Simulation analysis

The proposed modified adaptive NDI controller has been performed with a full nonlinear model. The reference trajectories of velocity, altitude and pitch angle are filtered through a second-order command filter.

$$V_{\text{ref}}/V_c = 0.03^2/\left(s^2 + 2\times0.95\times0.03s + 0.03^2\right)$$
$$h_{\text{ref}}/h_c = 0.03^2/\left(s^2 + 2\times0.95\times0.03s + 0.03^2\right) \quad (51)$$
$$\theta_{\text{ref}}/\theta_c = 1^2/\left(s^2 + 2\times1\times1s + 1^2\right)$$

The initial parameters of velocity and altitude are presented in Table 1, while the final parameters are chosen as V_c = 3002 m/s, h_c = 28956 m. The reference trajectory of pitch angle is $\theta_c = \gamma + \alpha_c$, where α_c = 2 deg. The flight envelope is listed in Table 2 to ensure the performance of the AHV. The control parameters are presented in Table 3. The model of the actuators is a second-order prototype representation. The damping ratio of all actuators is selected as 0.7. The natural frequency of the engine dynamics is 20 rad/s, while the elevator and canard have the natural frequencies 50 rad/s. The simulations are divided into two parts. The first part considers a comparison among the baseline NDI control, the modified adaptive NDI control, and the standard adaptive NDI control in the nominal state. The second part considers Monte Carlo evaluation to verify the tracking performance of the modified adaptive NDI control in the presence of parametric uncertainties.

The first part is mainly to verify the effectiveness of the adaptive scheme and the NDI control. Three cases are considered in the nominal state. Case 1: the baseline NDI control is verified, without the adaptive term. Case 2: the baseline NDI is enhanced with the modified adaptive scheme. Case 3: the baseline NDI is enhanced with the standard adaptive scheme that has the same adaptive gains with the modified adaptive scheme. Fig. 2 shows the first two cases can fulfill the tracking mission in the nominal state, which indicates the effectiveness of the NDI control. The standard adaptive scheme is divergent in the presence of high-gain learning rate. During the tracking process, the modified adaptive scheme based NDI has a good tracking performance, as presented in Fig. 3. The tracking errors of the baseline NDI control takes a relatively long time to converge to zeros.

The second part presents the Monte Carlo simulation results. A total of 100 times of Monte Carlo simulations are performed. The parameters ν_{21} and ν_{22} consider a uniform variation within 10% of the nominal value, while the parameters ν_1 to ν_{20} have a uniform variation within 20% of the nominal value. To illustrate the performance, only 20 second is presented.

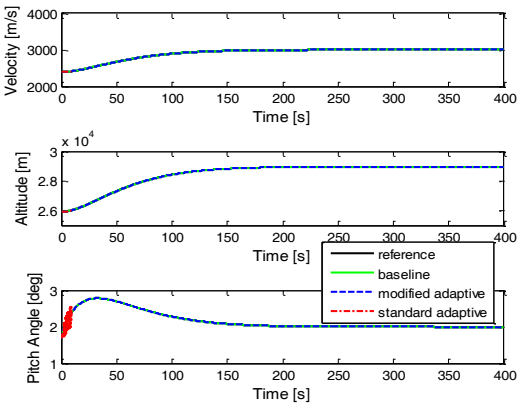

Figure 2. Trajectory tracking of the regulated states.

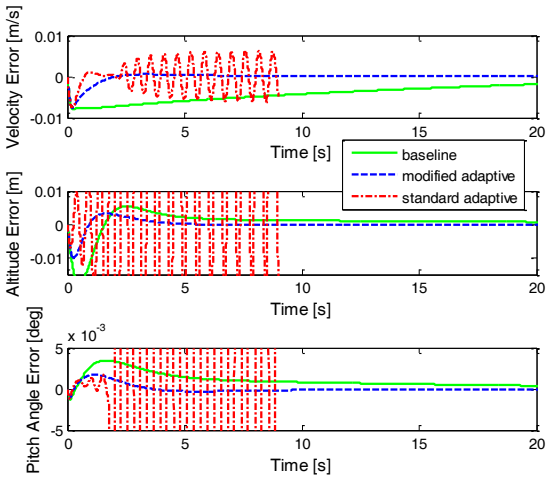

Figure 3. Trajectory tracking errors of the regulated states.

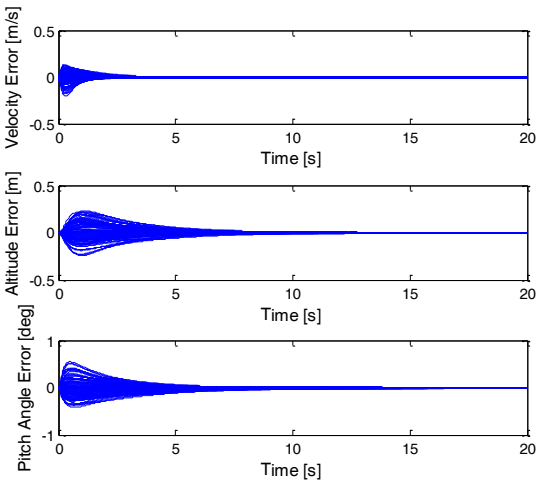

Figure 4. Trajectory tracking errors in the Monte Carlo simulation.

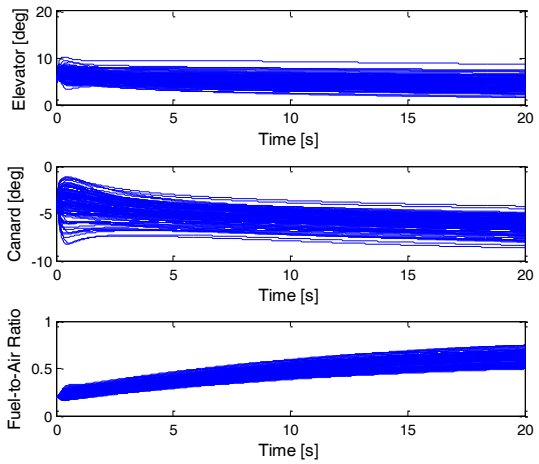

Figure 5. Control inputs in the Monte Carlo simulation.

Fig. 4 shows the modified adaptive scheme based NDI can fulfill the tracking mission in the presence of parametric uncertainties. The tracking errors converge to zeros within 10s in Fig. 4, and the control inputs are within the bounds in Fig. 5. Although the modified adaptive scheme adopts high gain learning rate, the high-frequency oscillations are cut off by the low-pass filter.

5. Conclusion

In this paper, we have designed a robust adaptive NDI control law for an AHV. The pole placement technique is applied to design the feedback gains of the equivalent linear system, which is convenient to set the gains for the clear physical meanings. The modified adaptive scheme applied a low-pass filter to cut off the high-frequency oscillations arising from the high-gain learning rate. The high gain learning rate of the modified adaptive scheme accelerates the convergence rate and is robust to parametric uncertainties. Simulation results show the effectiveness of the modified adaptive NDI control law, which provides a good tracking performance and a nice robust property for the AHV. The adaptive gains are chosen by trial and error. In the future work, we will study how to select the adaptive gains properly.

References

1. J.D. Shaughnessy, S.Z. Pinckney, J.D. McMinn, C.I. Cruz, M.-L. Kelley, Hypersonic vehicle simulation model: winged-cone configuration, 1990.
2. C. Bahm, E. Baumann, J. Martin, D. Bose, R. Beck, B. Strovers, The X-43A Hyper-X Mach 7 Flight 2 Guidance, Navigation, and Control Overview and Flight Test Results, AIAA/CIRA 13th International Space Planes and Hypersonics Systems and Technologies Conference, American Institute of Aeronautics and Astronautics, 2005.
3. M.K. Smart, N.E. Hass, A. Paull, Flight Data Analysis of the HyShot 2 Scramjet Flight Experiment, AIAA Journal, 44 (2006) 2366-2375.
4. M.A. Bolender, D.B. Doman, Nonlinear Longitudinal Dynamical Model of an Air-Breathing Hypersonic Vehicle, Journal of Spacecraft and Rockets, 44 (2007) 374-387.
5. Q. Wang, R.F. Stengel, Robust Nonlinear Control of a Hypersonic Aircraft, Journal of Guidance, Control, and Dynamics, 23 (2000) 577-585.
6. H. Xu, M.D. Mirmirani, P.A. Ioannou, Adaptive Sliding Mode Control Design for a Hypersonic Flight Vehicle, Journal of Guidance, Control, and Dynamics, 27 (2004) 829-838.
7. J.T. Parker, A. Serrani, S. Yurkovich, M.A. Bolender, D.B. Doman, Control-Oriented Modeling of an Air-Breathing Hypersonic Vehicle, Journal of Guidance, Control, and Dynamics, 30 (2007) 856-869.
8. C. Qi, A. Jianliang, NDI-Based L1 Adaptive Control Design for a Generic Hypersonic Vehicle Model, AIAA Guidance, Navigation, and Control Conference, American Institute of Aeronautics and Astronautics, 2017.
9. L. Fiorentini, A. Serrani, M.A. Bolender, D.B. Doman, Nonlinear Robust Adaptive Control of Flexible Air-Breathing Hypersonic Vehicles, Journal

of Guidance, Control, and Dynamics, 32 (2009) 402-417.
10. E. Lavretsky, R. Gadient, Robust Adaptive Design for Aerial Vehicles with State-Limiting Constraints, Journal of Guidance, Control, and Dynamics, 33 (2010) 1743-1752.
11. T. Yucelen, W.M. Haddad, Low-Frequency Learning and Fast Adaptation in Model Reference Adaptive Control, IEEE Transactions on Automatic Control, 58 (2013) 1080-1085.
12. D. Sigthorsson, P. Jankovsky, A. Serrani, S. Yurkovich, M. Bolender, D.B. Doman, Robust Linear Output Feedback Control of an Airbreathing Hypersonic Vehicle, Journal of Guidance, Control, and Dynamics, 31 (2008) 1052-1066.
13. L. Fiorentini, Nonlinear Adaptive Controller Design For Air-breathing Hypersonic Vehicles, The Ohio State University, 2010.
14. H.K. Khalil, Adaptive output feedback control of nonlinear systems represented by input-output models, IEEE Transactions on Automatic Control, 41 (1996) 177-188.
15. J.B. Pomet, L. Praly, Adaptive nonlinear regulation: estimation from the Lyapunov equation, IEEE Transactions on Automatic Control, 37 (1992) 729-740.